Regret and Climate Tipping Points*

Andrea Titton†

September 4, 2024

*I thank my supervisors Florian Wagener and Cees Diks for the patient guidance on this paper. I also thank Rick van der Ploeg, Christoph Hambel, and Frank Venmans for the insightful discussions. Finally, I thank attendees of the EEA-ESESM conference, Rotterdam, 2024 for the constructive comments.

†CeNDEF, Faculty of Economics and Business, University of Amsterdam a.titton@uva.nl

As the average world temperature rises, due to the emissions of greenhouse gases from human economic activities, positive feedbacks can push the climate system through critical thresholds, known as tipping points, into a regime of higher temperature. Reverting back the climate system to the current regime can be hard, if not impossible. This risk affects the trade-off between the economic gains from emissions and the damages such emissions impose on the economy. Unfortunately, there is a fundamental uncertainty around these tipping points. In this paper, I study the societal costs of late or insufficient abatement, driven by the misestimation of the tipping point and the climate system. To do so, I compute the socially optimal abatement policy in an integrated assessment model under three climate specification. A climate model with an imminent tipping point, one with a remote tipping point, and, finally, a climate model with stochastic tipping, as commonly used in the literature (see e.g. Hambel, Kraft and Schwartz 2021; Lemoine and Traeger 2016; Van Der Ploeg and De Zeeuw 2018). I then compute the social costs associated with being wrong: abating under the assumption of a remote tipping point or a stochastic tipping point, despite the tipping point being imminent.

1 Model

This section introduces the climate model and the economy.

1.1 Climate Model

1.1.1 CO_2 concentration and carbon sinks

Emissions from human economic activity E_t increase the average atmospheric concentration of CO_2 M_t. This, in turn, decays into natural sinks N_t. To model the saturation of natural sinks, the decay rate $\delta_m(N_t)$ falls in the quantity of carbon dioxide already stored in the natural sinks N_t. Hence, this evolves as

$$\xi_m \, \mathrm{d}N_t = \delta_m(N_t) M_t \; \mathrm{d}t \tag{1}$$

where ξ_m is a factor converting quantities from parts-per-million in volume to Gt of CO_2.

As we are concerned with abatement efforts, vis-à-vis a "business as usual" scenario, I rewrite variables in deviation from such scenario. Variables under business as usual are then calibrated using the IPCC SPSS5 projections (2023). Denote by E_t^b the emissions under such scenario, and by M_t^b and N_t^b the resulting carbon in the atmosphere and in natural sinks, respectively. The atmospheric concentration M_t^b under business as usual emissions evolves as

$$\frac{\mathrm{d}M_t^b}{M_t^b} = \gamma_t^b \,\mathrm{d}t + \sigma_m \,\mathrm{d}W_{m,t} \tag{2}$$

where

$$\gamma_t^b \coloneqq \xi_m \frac{E_t^b}{M_t^b} - \delta_m(N_t^b) \tag{3}$$

and $W_{m,t}$ is a Wiener process. The business as usual is chosen to be IPCC's SSP5 scenario (Kriegler et al., 2017). This scenario describes an energy intensive future, in which fossil fuel usage develops rapidly and little to no abatement takes place. Using this scenario, I then calibrate the implied growth rate of carbon concentration γ_t^b. Figure 1 shows the results of the calibration (Appendix C). The upper figure show s the path of the business as usual growth rate γ_t^b and the lower figure shows the implied growth of carbon concentration M_t^b. The carbon concentration in this scenario is assumed to grow at an increasingly fast rate until 2080, when the growth rate peaks at around 1.4%. Thereafter, the growth rate starts declining. Recall that γ_t^b is the growth rate of carbon concentration M_t^b, which is always positive, hence in the business as usual scenario, carbon concentration is always increasing.

Abatement efforts α_t lower the growth rate of carbon concentration M_t vis-à-vis the business as usual scenario M_t^b. Introduce the growth rate of carbon concentration $m_t \coloneqq \log M_t$. Then, its evolution is given by

$$\mathrm{d}m_t = \left(\gamma_t^b - \alpha_t\right) \mathrm{d}t + \sigma_m \,\mathrm{d}W_{m,t}\,. \tag{4}$$

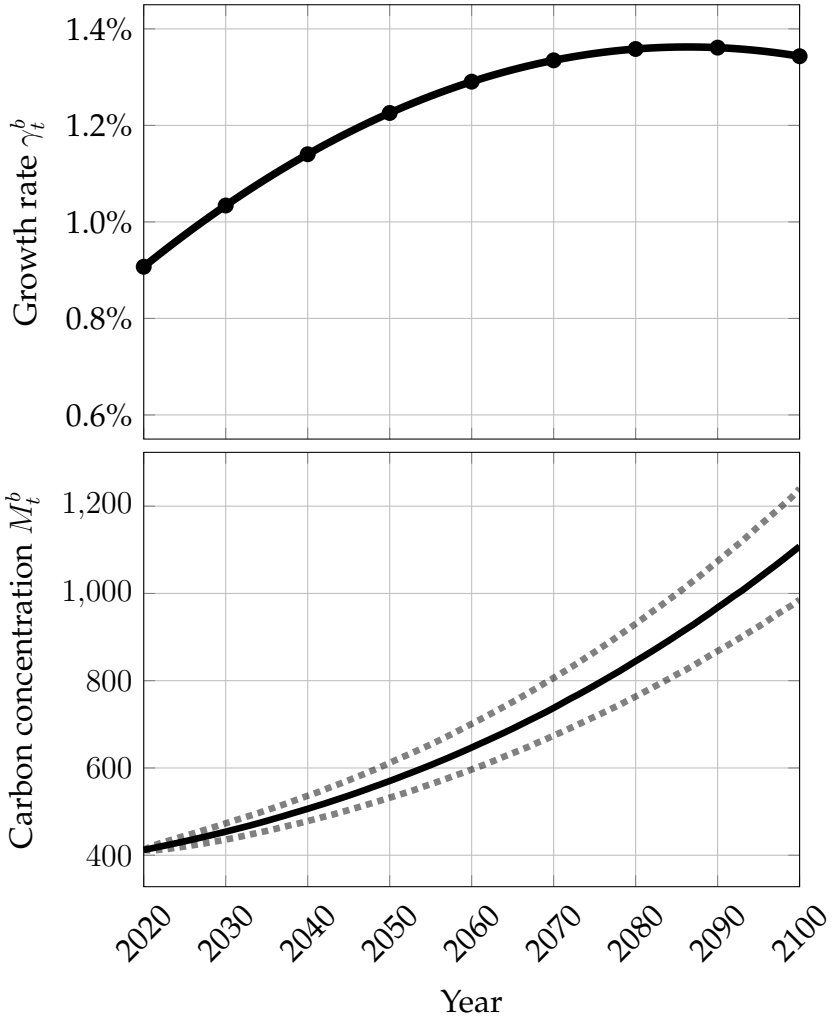

Figure 1: Growth rate of carbon concentration in the business as usual scenario γ_t^b and median path (solid) of business as usual carbon concentration M_t^b (2) with 5% and 95% confidence intervals (dashed).

By assumption, I assume that negative emissions are not attainable, namely

$$\alpha_t \leq \gamma_t^b + \delta_m(N_t). \tag{5}$$

This assumption is tested in Appendix (**?**). Implementing no abatement policy $\alpha_t = 0$ corresponds to a business as usual scenario $M_t \equiv M_t^b$, while implementing a full abatement policy $\alpha_t = \gamma_t^b$ stabilises carbon concentration. Any abatement policy α_t can be implicitly linked back to the corresponding level of emissions by introducing an emission reduction rate $\varepsilon(\alpha_t)$, which keeps tracks of what percentage of emission has been abated

$$E_t = \big(1 - \varepsilon(\alpha_t)\big) E_t^b. \tag{6}$$

1.1.2 Temperature

Earth's radiating balance, in its simplest form, prescribes that an equilibrium temperature $\bar{T}$ is determined by equating incoming solar radiation S with outgoing long-wave radiations $\eta\sigma\bar{T}^4$, where σ is the Stefan-Boltzmann constant and η is an emissivity rate. Due to the presence of greenhouse gasses, certain wavelengths are scattered and, hence, not emitted[1]. This introduces an additional radiative forcing G which yields the balance equation $S = \eta\sigma\bar{T}^4 - G$. Focusing on the role of increased CO_2, as opposed to other greenhouse gases, we can decompose the greenhouse radiative forcing term G into a constant component G_0 and a component which depends on the steady state level of CO_2 concentration in the atmosphere M_t with respect to the pre-industrial level M^p, such that

$$G \equiv G_0 + G_1 \log(M_t/M^p) = G_0 + G_1 \left(m_t - m_t^p\right). \tag{7}$$

I introduce a feedback in the temperature by assuming that the absorbed incoming solar radiation is increasing in temperature. This choice can be seen as a stylised model of the ice-albedo feedback (Ashwin et al., 2012; McGuffie and

[1] See Ghil and Childress (2012) and Greiner and Semmler (2005) for a more detailed discussion.

Henderson-Sellers, 2005), yet, any positive feedback in temperature dynamics would yield similar interpretations. The incoming solar radiation S can be then decomposed into $S_0\left(1-\lambda(T_t)\right)$ where the function $\lambda(T_t)$ transitions from a higher λ_1 to a lower level $\lambda_1-\Delta\lambda$ via a smooth transition function $L(T_t)$. To control at which level of temperature the transition occurs the transition functions take the form

$$\lambda(T_t) \coloneqq \lambda_1 - \Delta\lambda\big(1-L(T_t)\big) \text{ with} \tag{8a}$$

$$L(T_t) \coloneqq \frac{1}{1+\exp\left(-L_1\left(T_t - T^p - T^c - \frac{\Delta T}{2}\right)\right)} \tag{8b}$$

where T^p is the pre-industrial level of temperature, T^c is the level of temperature at which the feedback effect begins, ΔT is the duration of the transition, and L_1 is a speed parameter.

The costs that society incurs if it behaves under the wrong assumption over T^c are the focus of the subsequent sections. Best estimates from climate sciences are that many such transitions occur for average global temperatures between $1.5°$ and $3°$ over pre-industrial levels (Seaver Wang et al., 2023). Yet, there is large uncertainty around these variables. Ben-Yami et al. (2024) show that the uncertainty is so large that estimating critical thresholds T^c from historical data is unfeasible. In this paper, I consider two extreme scenarios: one in which the tipping point is *imminent* $T^c = 1.5°$ and one in which it is *remote* $T^c = 2.5°$. The parameter $\Delta\lambda$ is calibrated by matching a climate sensitivity, that is, the expected equilibrium temperature of doubling CO_2 concentration $M_t = 2M^p$, of $4.5°$, which is the upper end of the range deemed very likely in the AR6 Calvin et al. (2023). Figure 2 shows the transition function (8) under these two scenarios. Despite being a highly stylised average model for a complex and spatially heterogeneous process, λ captures the core mechanism behind feedback processes in the temperature dynamics. Putting these processes together we can write the two determinants of temperature dynamics: radiative forcing, which

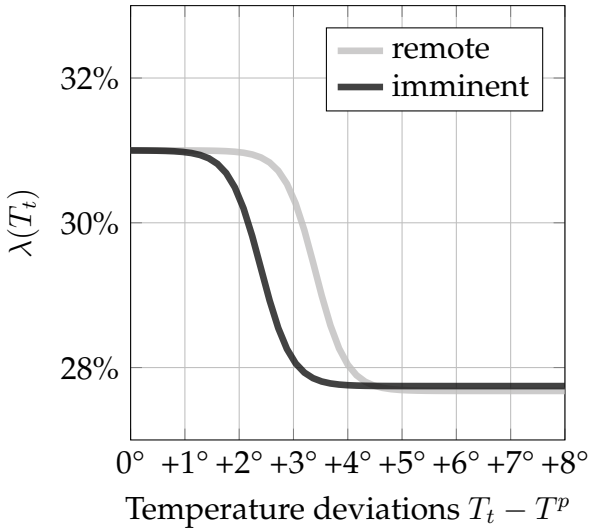

Figure 2: Coefficient $\lambda(T)$ for different threshold temperatures $T^c \in \{1.5, 3.5\}$

only depends on temperature,

$$r(T_t) \coloneqq S_0 \left(1 - \lambda(T_t)\right) - \eta\sigma T_t^4 \tag{9}$$

and the greenhouse gasses effects, which only depends on the log deviation of atmospheric carbon concentration with respect to its pre-industrial levels,

$$g(m_t) \coloneqq G_0 + G_1(m_t - m^p). \tag{10}$$

Putting these two drivers together we can write temperature deviations as

$$\epsilon \, \mathrm{d}T_t = r(T_t) \, \mathrm{d}t + g(m_t) \, \mathrm{d}t + \sigma_T \, dW_{T,t}, \tag{11}$$

where ϵ is the thermal inertia and $W_{T,t}$ is a Wiener process.

1.1.3 Tipping Points

The presence of the feedback effect λ introduces tipping points in the temperature dynamics. This is illustrated in Figure 3 for a critical temperature $T^c = 2°$. For a given level of carbon concentration $\bar{M}$, the temperature $\bar{T}$ tends towards a steady state satisfying $\mathbb{E}\,\mathrm{d}T_t = 0$ or equivalently $r(\bar{T}) = -g(\bar{m})$ where

$\bar{m} = \log \bar{M}$ (solid line). For low values of carbon concentration $\bar{M} \lesssim 350$, such

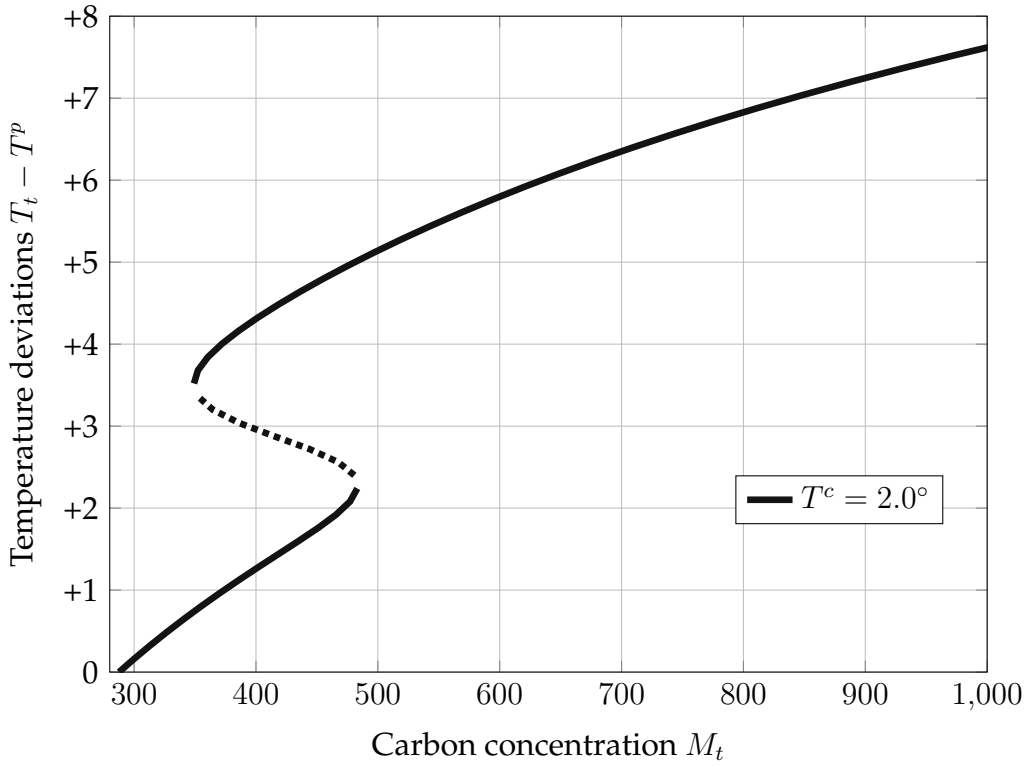

Figure 3: Steady states of temperature T_t and carbon concentration M_t for $T^c = 2°$. The solid and dashed lines represent attracting and repelling steady states, respectively.

steady state is unique. As more carbon dioxide gets added to the atmosphere, two additional steady state levels of temperature $\bar{T}$ arise, one stable (upper solid line) and one separating unstable (dashed line). The presence of the additional steady state is hard to detect as the relationship between temperature T_t and carbon concentration M_t is still log-linear. This makes estimating the presence of a tipping point and its threshold T^c complicated. As carbon concentration increases further $M_t \gtrsim 490$ and temperature crosses the critical threshold T^c, the old stable and low temperature regime is not feasible any more and only a high stable temperature regime remains. Any increase of carbon concentration at this tipping point would then lead to a rapid increase in temperature to a this new steady state. Crucially, to revert the system back to the lower temperature regime, it is not sufficient to remove just the carbon that caused the system to tip, but society would have to remove all carbon until the only stable steady state is the low temperature, hence back to $M_t \lesssim 350$ ("walking

along" the upper solid line). In the context of the example of an ice-albedo tipping point, at low level of carbon concentration the Earth's ice coverage is large and the albedo coefficient, that is, the percentage of solar radiation reflected by the lighter coloured surface. As temperature rises, and ice melts, the albedo decreases, which further contributes to temperature increases. This positive feedback might push the world into an "ice-free" regime with low albedo. To restore ice coverage temperature must decrease further than the increase of the tipping point.

Figure 4 displays how this mechanism impacts the dynamics of temperature under the business as usual scenario for a critical thresholds T^c of $2°$ (darker) and $3.5°$ (lighter). The lines with the markers show a simulation of temperature T_t (11) and carbon concentration M_t under business as usual (2). Markers denotes the temperature and carbon concentration every 10 years starting from 2020. For the first three decades, the temperature dynamics are identical. Then suddenly, if the tipping point is closer $T^c = 2°$, temperature grows rapidly to the new steady state and, in 20 years, the system converges to a high temperature regime, before the log-linear relationship between temperature T_t and carbon concentration M_t is established again. This occurs much later whenever the critical temperature T^c, and hence the tipping point, are higher. Given the high uncertainty behind T^c and the resulting different temperature dynamics, after introducing the economy in the next section, the paper focuses on the optimal abatement efforts under different levels of T^c and the costs associated with wrongly estimating it.

1.2 Economy

1.2.1 Capital and Climate Damages

Output Y_t is the product of the capital stock K_t and its productivity A_t

$$Y_t \coloneqq A_t K_t. \tag{12}$$

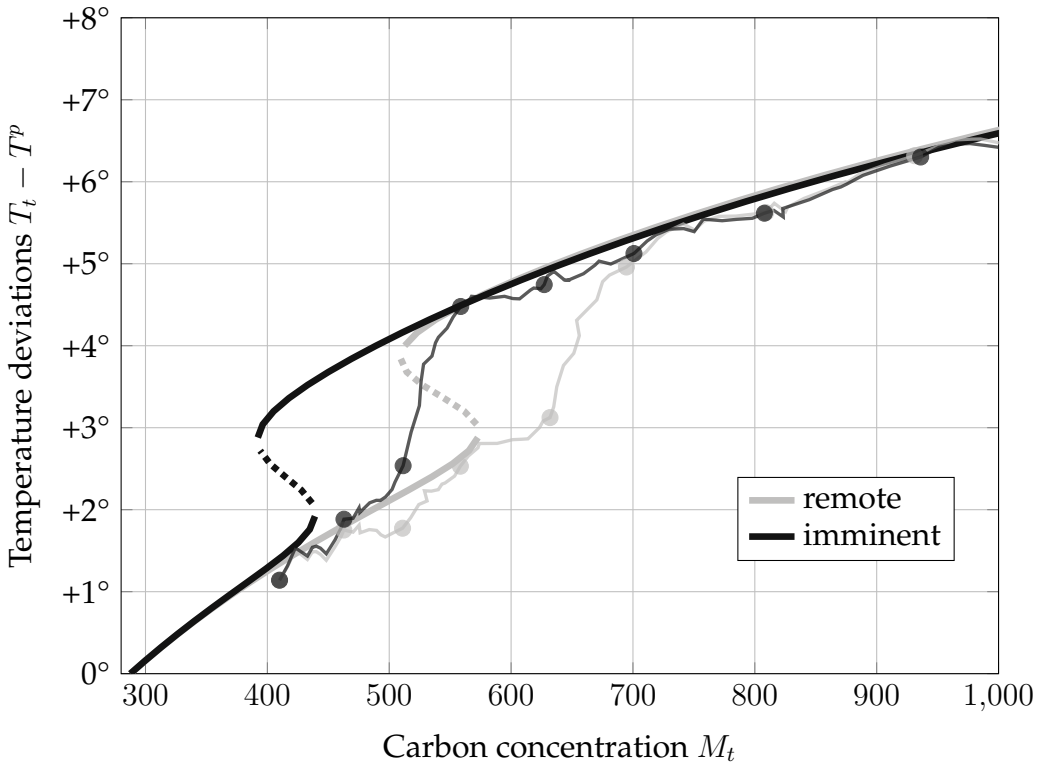

Figure 4: Steady states of temperature T_t and carbon concentration M_t for $T^c = 2°$ (dark) and $T^c = 3°$ (light). The solid and dashed lines represent attracting and repelling steady states, respectively. The marked line show two simulation of temperature and carbon concentration under the business as usual scenario. Markers denotes the temperature and carbon concentration every 10 years starting from 2020.

Productivity is assumed to grow at a constant rate ϱ. Output Y_t can be used for investment in capital I_t, abatement expenditures B_t, or consumption C_t, imposing the constraint

$$Y_t = I_t + B_t + C_t. \tag{13}$$

In absence of climate change, K_t depreciates at a rate δ_k but can be substituted by capital investments I_t, which incurs, along with abatement expenditure B_t, in quadratic adjustment costs

$$\frac{\kappa}{2}\left(\frac{I_t + B_t}{K_t}\right)^2 K_t. \tag{14}$$

Climate change interacts with the economy by lowering capital growth via damages $d(T_t)$ which are increasing in temperature T_t. Following Weitzman (2012), I assume the damage function to take the form

$$d(T_t) \coloneqq \xi \, (T_t - T^p)^{\upsilon} \tag{15}$$

where T^p is the pre-industrial level of temperature (Figure 5).

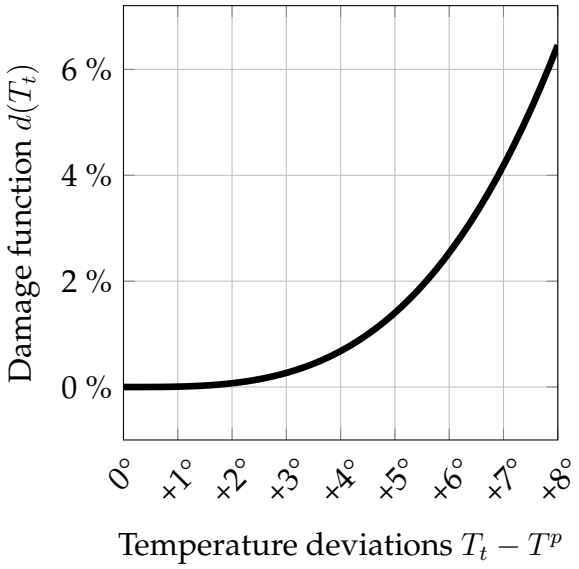

Figure 5: Damage function with the Weitzman (2012) calibration.

This stylised form captures the empirical evidence that under higher temperature levels some forms of capital, particularly in the agricultural (Dietz and

Lanz, 2019) or manufacturing sectors (Dell, Jones and Olken, 2009), become more expensive or harder to substitute. A common alternative in the literature is to assume that higher temperatures wipe out part of the capital stocks (Nordhaus, 1992). The comparison between these two assumption is carried out in Appendix (**?**) and a thorough treatment can be found in (Hambel, Kraft and Schwartz, 2021).

Putting the endogenous growth of capital and the climate damages together, the growth rate of capital satisfies

$$\frac{\mathrm{d}K_t}{K_t} = \left(\frac{I_t}{K_t} - \delta_k - \frac{\kappa}{2} \left(\frac{I_t + B_t}{K_t} \right)^2 \right) \mathrm{d}t - d(T_t)\,\mathrm{d}t + \sigma_k\,\mathrm{d}W_k\,, \tag{16}$$

where W_k is a Weiner process.

In the following, I link the abatement costs B_t with the abatement rate α_t, introduced in the previous section. Introduce $\beta \coloneqq B_t/Y_t$ the fraction of output devoted to abatement. As in Nordhaus (1992), I assume this to be quadratic function of the fraction of abated emissions $\varepsilon(\alpha_t)$ (6), namely,

$$\beta_t(\varepsilon(\alpha_t)) = \frac{\omega_t}{2}\,\varepsilon(\alpha_t)^2. \tag{17}$$

Under this assumption, no abatement is free, as $\beta_t(0) = 0$. At a fixed time t, higher abatement rates α_t and hence higher emission reduction $\varepsilon(\alpha_t)$ vis-a-vis the business as usual scenario, become increasingly costly at a rate $\omega_t\varepsilon(\alpha_t)$. As time progresses, so does abatement technology and a given abatement objective becomes cheaper. This is modelled by letting the exogenous technological parameter ω_t decrease over time. There is large uncertainty around the path of ω_t.

Let

$$\chi_t \coloneqq \frac{C_t}{Y_t} \tag{18}$$

be the fraction of output devoted to consumption. Using the budget constraint (13) and the two controls α_t and χ_t, the growth rate of capital (16) can be rewrit-

ten as

$$\frac{\mathrm{d}K_t}{K_t} = \Big(\phi_t(\chi_t) - A_t\beta_t(\varepsilon(\alpha_t)) - d(T_t)\Big)\,\mathrm{d}t + \sigma_k\,\mathrm{d}W_{k,t} \tag{19}$$

where

$$\phi_t(\chi_t) \coloneqq A_t(1-\chi_t) - \frac{\kappa}{2}A_t^2(1-\chi_t)^2 - \delta_k \tag{20}$$

is an endogenous growth component, $\beta_t(\varepsilon(\alpha_t))$ is the fraction of output allocated to abatement for an abatement rate α_t, and $d(T_t)$ are the damages from climate change. This formulation makes the trade-off between climate abatement and economic growth apparent. Devoting fewer resources to abatement to pursue higher capital, and hence, output growth, yields higher future temperature and can put the economy in a lower growth path altogether.

Finally, as output Y_t is just the product of capital K_t and productivity A_t, its growth rate differs from that of capital just by the growth rate of productivity, hence it satisfies

$$\frac{\mathrm{d}Y_t}{Y_t} = \varrho + \frac{\mathrm{d}K_t}{K_t}. \tag{21}$$

2 Social Planner Problem and Regret

This section introduces the objective of the social planner and the resulting maximisation problem. Societal utility at time t given a state $X_t \coloneqq (T_t, M_t, N_t, Y_t)$ is recursively defined as

$$V_t(X_t) = \sup_{\chi,\alpha} \mathbb{E}_t \int_t^\infty f(\chi_s(X_s)Y_s, V_s(X_s))\,\mathrm{d}s \tag{22}$$

where χ and α are continuous functions over time and the state space, and f is an Epstein-Zin aggregator

$$f(c,u) \coloneqq \frac{\rho}{1-1/\psi}(1-\theta)u\left(\left(\frac{c}{((1-\theta)u)^{\frac{1}{1-\theta}}}\right)^{1-1/\psi} - 1\right). \tag{23}$$

Consumption is integrated into a utility index by means of the Epstein-Zin integrator (Duffie and Epstein, 1992). This aggregator plays a dual role. First, it al-

lows to disentangle the role of relative risk aversion θ, elasticity of intertemporal substitution ψ and the discount rate ρ in determining optimal abatement paths. Second, it circumvents the known paradoxical result that abatement policies becomes less ambitious as society becomes more risk averse (Pindyck and Wang, 2013). Details on solving the problem (22) are given in Appendix B.

The paths of consumption and climate abatement resulting from the maximisation problem are then the optimal consumption and abatement paths.

3 Results

This section presents the optimal policies and the regret under three different scenarios. First, the case of an *imminent* tipping point, $T^c = 1.5°$. Second, the case of a *remote* tipping point, $T^c = 2.5°$. Third, the case of the literature *benchmark* stochastic tipping model (as described in Appendix D).

3.1 Optimal Abatement

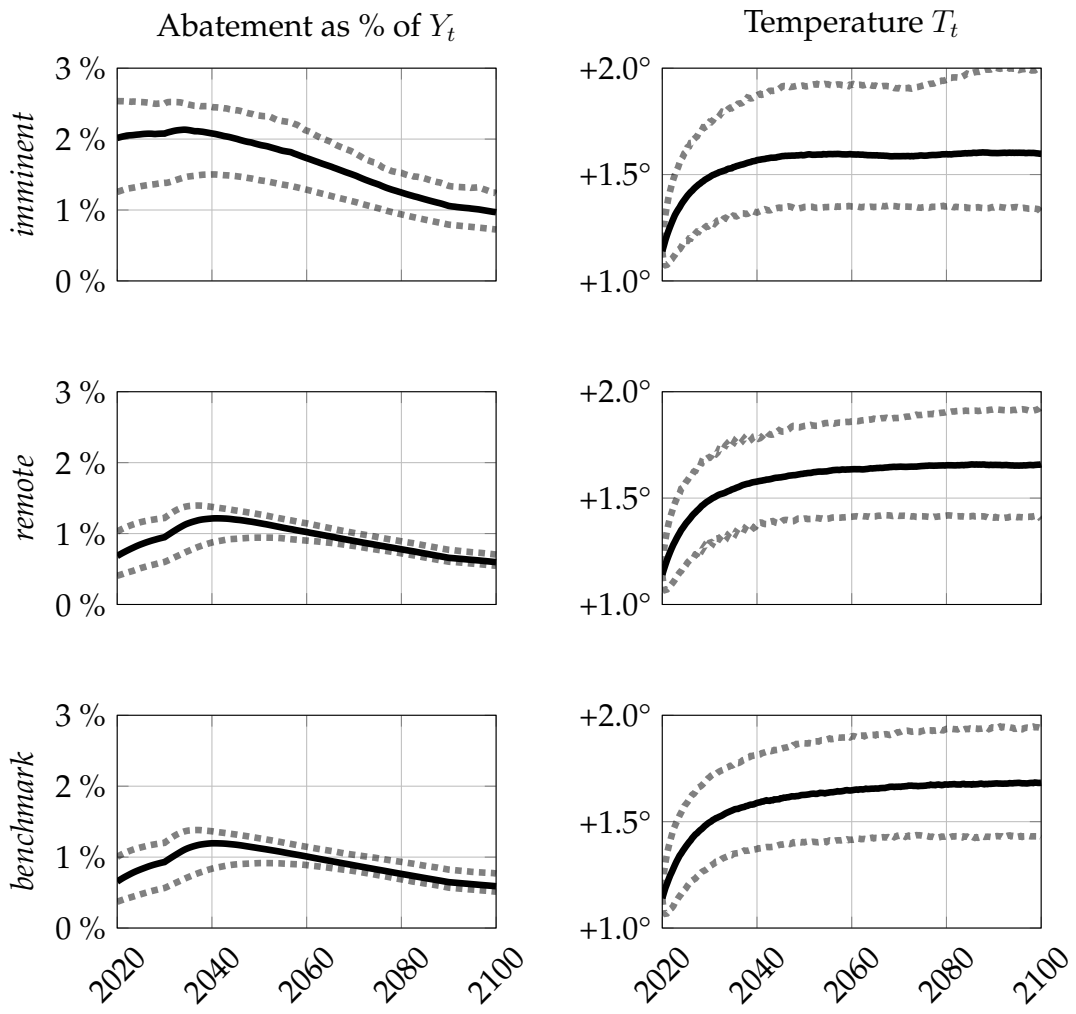

Figure 6: Optimal abatement expenditure β_t as a fraction of GDP and resulting temperature dynamics for the three modelling specifications. The confidence intervals show the 1st and 99th quantiles of 10000 simulations.

3.2 Regret

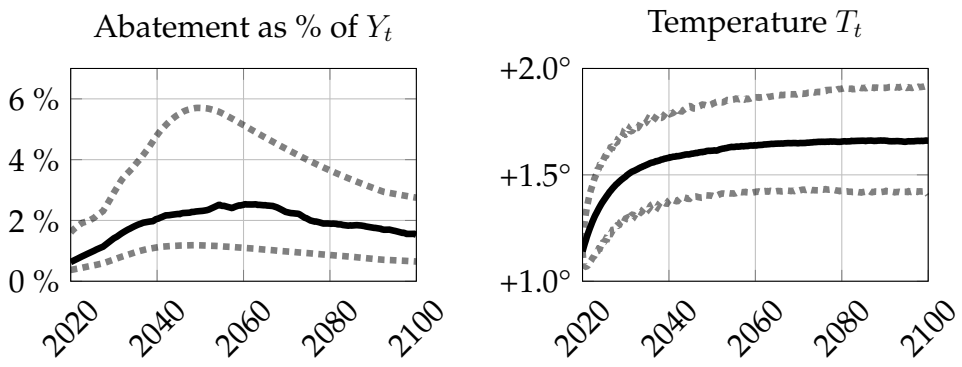

Figure 7: Abatement expenditure β_t as a fraction of GDP and resulting temperature dynamics associated with using the optimal abatement in the remote case until $T > T^c$ and that of the imminent case thereafter, with the dynamics implied by an imminent tipping point. The confidence intervals show the 1st and 99th quantiles of 10000 simulations.

4 Conclusion

This paper studies the role of tipping points in determining optimal emissions. Building on the calibration by Hambel, Kraft and Schwartz (2021), I extend the climate dynamics to include a potential bifurcation induced by the loss in albedo due to the change in the area of ice caps, sea ice, and glaciers Ashwin and Von Der Heydt (2020); Ashwin et al. (2012). I show that, in the presence of tipping points, optimal abatement is more ambitious in scope and timing. In fact, early abatement is crucial to avoid long periods of exposure to tipping risk.

The model presented here represents an early and simplified analysis that can be extended in various directions. First, more work is needed to analytically link the risk of tipping and the optimal abatement strategy, in order to quantify precisely the role of higher order climate dynamics in determining the social cost of carbon. Second, the underlying assumption of the social planner's optimisation problem is that she knows the climate dynamics and the role of the ice-albedo feedback. Such an assumption calls for extending the analysis to a situation in which the magnitude of the albedo loss is not known and rather can be estimated using early warning signals. Yet, in the face of uncertainty, the optimal abatement policy derived in this paper serves as a good rule against the possible worst case scenario.

References

Ackerman, Frank, Elizabeth A. Stanton, and Ramón Bueno. 2013. "Epstein–Zin Utility in DICE: Is Risk Aversion Irrelevant to Climate Policy?" *Environmental and Resource Economics*, 56(1): 73–84. 28

Ashwin, Peter, and Anna S. Von Der Heydt. 2020. "Extreme Sensitivity and Climate Tipping Points." *Journal of Statistical Physics*, 179(5-6): 1531–1552. 17

Ashwin, Peter, Sebastian Wieczorek, Renato Vitolo, and Peter Cox. 2012. "Tipping points in open systems: bifurcation, noise-induced and rate-dependent examples in the climate system." *Philosophical Transactions of the Royal Society A: Mathematical, Physical and Engineering Sciences*, 370(1962): 1166–1184. 5, 17

Ben-Yami, Maya, Andreas Morr, Sebastian Bathiany, and Niklas Boers. 2024. "Uncertainties too large to predict tipping times of major Earth system components from historical data." *Science Advances*, 10(31): eadl4841. 6

Calvin, Katherine, Dipak Dasgupta, Gerhard Krinner, Aditi Mukherji, Peter W. Thorne, Christopher Trisos, José Romero, Paulina Aldunce, Ko Barrett, Gabriel Blanco, William W.L. Cheung, Sarah Connors, Fatima Denton, Aïda Diongue-Niang, David Dodman, Matthias Garschagen, Oliver Geden, Bronwyn Hayward, Christopher Jones, Frank Jotzo, Thelma Krug, Rodel Lasco, Yune-Yi Lee, Valérie Masson-Delmotte, Malte Meinshausen, Katja Mintenbeck, Abdalah Mokssit, Friederike E.L. Otto, Minal Pathak, Anna Pirani, Elvira Poloczanska, Hans-Otto Pörtner, Aromar Revi, Debra C. Roberts, Joyashree Roy, Alex C. Ruane, Jim Skea, Priyadarshi R. Shukla, Raphael Slade, Aimée Slangen, Youba Sokona, Anna A. Sörensson, Melinda Tignor, Detlef Van Vuuren, Yi-Ming Wei, Harald Winkler, Panmao Zhai, Zinta Zommers, Jean-Charles Hourcade, Francis X. Johnson, Shonali Pachauri, Nicholas P. Simpson, Chandni Singh, Adelle Thomas, Edmond Totin, Paola Arias, Mercedes Bustamante, Ismail Elgi-

zouli, Gregory Flato, Mark Howden, Carlos Méndez-Vallejo, Joy Jacqueline Pereira, Ramón Pichs-Madruga, Steven K. Rose, Yamina Saheb, Roberto Sánchez Rodríguez, Diana Ürge Vorsatz, Cunde Xiao, Noureddine Yassaa, Andrés Alegría, Kyle Armour, Birgit Bednar-Friedl, Kornelis Blok, Guéladio Cissé, Frank Dentener, Siri Eriksen, Erich Fischer, Gregory Garner, Céline Guivarch, Marjolijn Haasnoot, Gerrit Hansen, Mathias Hauser, Ed Hawkins, Tim Hermans, Robert Kopp, Noëmie Leprince-Ringuet, Jared Lewis, Debora Ley, Chloé Ludden, Leila Niamir, Zebedee Nicholls, Shreya Some, Sophie Szopa, Blair Trewin, Kaj-Ivar Van Der Wijst, Gundula Winter, Maximilian Witting, Arlene Birt, Meeyoung Ha, José Romero, Jinmi Kim, Erik F. Haites, Yonghun Jung, Robert Stavins, Arlene Birt, Meeyoung Ha, Dan Jezreel A. Orendain, Lance Ignon, Semin Park, Youngin Park, Andy Reisinger, Diego Cammaramo, Andreas Fischlin, Jan S. Fuglestvedt, Gerrit Hansen, Chloé Ludden, Valérie Masson-Delmotte, J.B. Robin Matthews, Katja Mintenbeck, Anna Pirani, Elvira Poloczanska, Noëmie Leprince-Ringuet, and Clotilde Péan. 2023. "IPCC, 2023: Climate Change 2023: Synthesis Report. Contribution of Working Groups I, II and III to the Sixth Assessment Report of the Intergovernmental Panel on Climate Change [Core Writing Team, H. Lee and J. Romero (eds.)]. IPCC, Geneva, Switzerland." Intergovernmental Panel on Climate Change (IPCC). Edition: First. 6

Crost, Benjamin, and Christian P. Traeger. 2013. "Optimal climate policy: Uncertainty versus Monte Carlo." *Economics Letters*, 120(3): 552–558. 28

Dell, Melissa, Benjamin F Jones, and Benjamin A Olken. 2009. "Temperature and Income: Reconciling New Cross-Sectional and Panel Estimates." *American Economic Review*, 99(2): 198–204. 12

Dietz, Simon, and Bruno Lanz. 2019. "Growth and adaptation to climate change in the long run." IRENE Institute of Economic Research IRENE Working Papers 19-09. 11

Duffie, Darrell, and Larry G. Epstein. 1992. "Asset Pricing with Stochastic Differential Utility." *Review of Financial Studies*, 5(3): 411–436. 13

Epstein, Larry G., and Stanley E. Zin. 1989. "Substitution, Risk Aversion, and the Temporal Behavior of Consumption and Asset Returns: A Theoretical Framework." *Econometrica*, 57(4): 937. 27

Ghil, Michael, and Stephen Childress. 2012. *Topics in geophysical fluid dynamics: atmospheric dynamics, dynamo theory, and climate dynamics.* Vol. 60, Springer Science & Business Media. 5

Greiner, Alfred, and Willi Semmler. 2005. "Economic growth and global warming: A model of multiple equilibria and thresholds." *Journal of Economic Behavior & Organization*, 57(4): 430–447. 5

Hambel, Christoph, Holger Kraft, and Eduardo Schwartz. 2021. "Optimal carbon abatement in a stochastic equilibrium model with climate change." *European Economic Review*, 132: 103642. 2, 12, 17, 23, 30

Intergovernmental Panel On Climate Change. 2023. *Climate Change 2021 – The Physical Science Basis: Working Group I Contribution to the Sixth Assessment Report of the Intergovernmental Panel on Climate Change.* . 1 ed., Cambridge University Press. 3

Kriegler, Elmar, Nico Bauer, Alexander Popp, Florian Humpenöder, Marian Leimbach, Jessica Strefler, Lavinia Baumstark, Benjamin Leon Bodirsky, Jérôme Hilaire, David Klein, Ioanna Mouratiadou, Isabelle Weindl, Christoph Bertram, Jan-Philipp Dietrich, Gunnar Luderer, Michaja Pehl, Robert Pietzcker, Franziska Piontek, Hermann Lotze-Campen, Anne Biewald, Markus Bonsch, Anastasis Giannousakis, Ulrich Kreidenweis, Christoph Müller, Susanne Rolinski, Anselm Schultes, Jana Schwanitz, Miodrag Stevanovic, Katherine Calvin, Johannes Emmerling, Shinichiro Fujimori, and Ottmar Edenhofer. 2017. "Fossil-fueled development (SSP5):

An energy and resource intensive scenario for the 21st century." *Global Environmental Change*, 42: 297–315. 3

Kushner, Harold J., and Paul Dupuis. 2001. *Numerical Methods for Stochastic Control Problems in Continuous Time.* Vol. 24 of *Stochastic Modelling and Applied Probability*, New York, NY:Springer New York. 26, 27

Lemoine, Derek, and Christian P. Traeger. 2016. "Ambiguous tipping points." *Journal of Economic Behavior & Organization*, 132: 5–18. 2

Lontzek, Thomas S., Yongyang Cai, Kenneth L. Judd, and Timothy M. Lenton. 2015. "Stochastic integrated assessment of climate tipping points indicates the need for strict climate policy." *Nature Climate Change*, 5(5): 441–444. 28

McGuffie, Kendal, and Ann Henderson-Sellers. 2005. *A Climate Modelling Primer.* . 1 ed., Wiley. 5

Nordhaus, William D. 1992. "An optimal transition path for controlling greenhouse gases." *Science*, 258(5086): 1315–1319. 12

Nordhaus, William D. 2014. "Estimates of the Social Cost of Carbon: Concepts and Results from the DICE-2013R Model and Alternative Approaches." *Journal of the Association of Environmental and Resource Economists*, 1(1): 273–312. 28

Nordhaus, William D. 2017. "Revisiting the social cost of carbon." *Proceedings of the National Academy of Sciences of the United States of America*, 114(7): 1518–1523. 28

Pindyck, Robert S, and Neng Wang. 2013. "The Economic and Policy Consequences of Catastrophes." *American Economic Journal: Economic Policy*, 5(4): 306–339. 14

Seaver Wang, A. Foster, E. A. Lenz, J. Kessler, J. Stroeve, L. Anderson, M. Turetsky, R. Betts, Sijia Zou, W. Liu, W. Boos, and Z. Hausfather. 2023.

"Mechanisms and Impacts of Earth System Tipping Elements." *Reviews of Geophysics*. S2ID: 41df6f88eb3d307fe0a68799909c900206988e6e. 6

Van Der Ploeg, Frederick, and Aart De Zeeuw. 2018. "Climate Tipping and Economic Growth: Precautionary Capital and the Price of Carbon." *Journal of the European Economic Association*, 16(5): 1577–1617. 2

Weitzman, Martin L. 2012. "GHG Targets as Insurance against Catastrophic Climate Damages." *Journal of Public Economic Theory*, 14(2): 221–244. 11

A Distribution of temperature

This section derives the steady state density of temperature given a fixed carbon concentration. The density is then use to calibrate the climate sensitivity and the initial conditions.

The Fokker-Planck equation for the density of temperature p_t is

$$\partial_T \left\{ \frac{\mu(T,m)}{\epsilon}\, p_t(T) + \frac{1}{2}\left(\frac{\sigma_T}{\epsilon}\right)^2 p_t'(T) \right\} = 0. \tag{24}$$

The steady state temperature $\overline{p}$ then satisfies the differential equation

$$\frac{\mu(T,m)}{\epsilon}\, \overline{p}(T) + \frac{1}{2}\left(\frac{\sigma_T}{\epsilon}\right)^2 \overline{p}'(T) = 0. \tag{25}$$

One can readily checked that this is solved by

$$\overline{p}(T) \propto \exp\left(-\frac{V(T,m)}{\sigma_T^2/2\epsilon^2}\right), \tag{26}$$

where

$$\begin{aligned} V(T,m) &\coloneqq g(m)T + \int r(T)\,\mathrm{d}T \\ &= g(m)T + S_0(1-\lambda_1)T - \frac{\eta}{5}T^5 + S_0\Delta\lambda\log(1+\exp(T-T_i)). \end{aligned} \tag{27}$$

B Solution to Maximisation

This appendix deals with the solution of the maximisation problem (22).

B.1 Simplifying Assumptions on the Decay Rate of Carbon

To reduce the state space, following Hambel, Kraft and Schwartz (2021), I make an assumption on the decay rate of carbon. The calibrated carbon decay δ_m, as a function of the carbon stored in sinks N_t, is illustrated in Figure 8. The

calibration assumes a functional form

$$\delta_m(N_t) = a_\delta e^{-\left(\frac{N_t - c_\delta}{b_\delta}\right)^2}, \tag{28}$$

for parameters $a_\delta, b_\delta, c_\delta$.

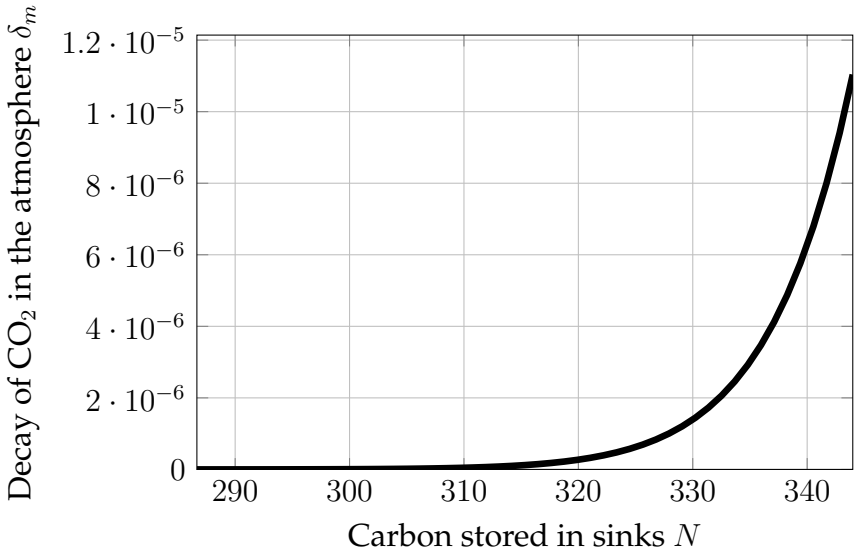

Figure 8: Estimated decay of carbon δ_m as a function of the carbon stored in sinks N_t.

I assume that the amount of carbon sinks present in the atmosphere is a constant fraction of the concentration in the atmosphere, $N_t = \frac{N_0}{M_0} M_t$. Abusing notation, I henceforth write $\delta_m(M_t)$ for the decay rate. Using this setup, under a business-as-usual emission scenario, the decay of carbon follows the path in Figure 9.

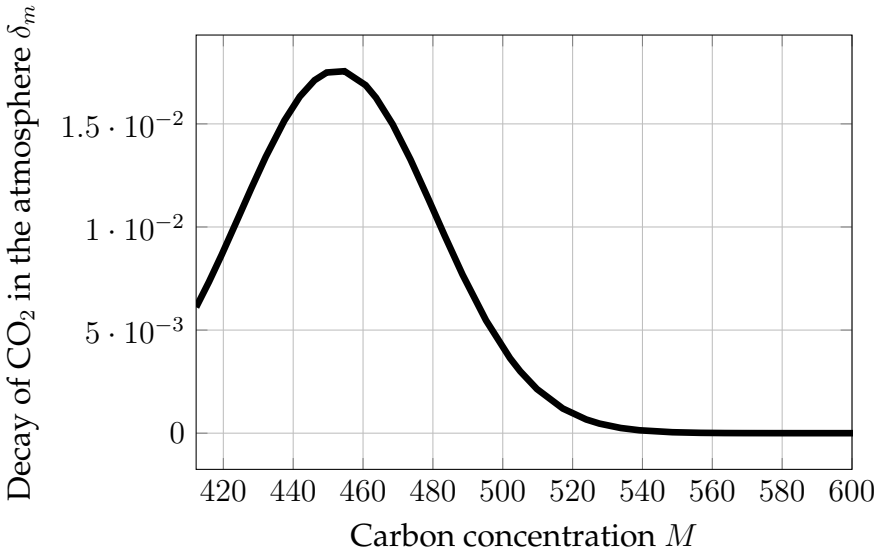

Figure 9: Estimated decay of carbon δ_m under the business as usual emission scenario M^b. Each marker is the decay after every decade.

B.2 Hamilton-Jacobi-Bellman equation

Using the assumption from Appendix B.1, the value function V at time t depends only on temperature T_t, log-carbon concentration m_t and output Y_t. This satisfies the Hamilton-Jacobi-Bellman equation

$$\begin{aligned} -\partial_t V = \sup_{\chi,\alpha} & f(\chi Y, V) + \partial_m V \ (\gamma_t^b - \alpha) + \partial_m^2 V \ \frac{\sigma_m^2}{2} \\ & + \partial_Y V(\varrho + \phi(\chi) - d(T) - \beta_t(\varepsilon(\alpha))) + \partial_k^2 V \ \frac{\sigma_Y^2}{2} \\ & + \partial_T V \ \frac{r(T) + g(m)}{\epsilon} + \partial_T^2 V \ \frac{(\sigma_T/\epsilon)^2}{2}. \end{aligned} \tag{29}$$

It is easy to check that the ansatz

$$V_t(T, m, Y) = \frac{Y^{1-\theta}}{1-\theta} F_t(T, m) \tag{30}$$

satisfies (29).

B.3 Approximating Markov Chain

The Hamilton-Jacobi-Bellman equation (29) is solved for F by adapting the method proposed in Kushner and Dupuis (2001). The idea is to discretise the state space of T and m and compute time dependent intervals $\Delta t(T, m)$. Then, constructing a Markov chain $\mathcal{M}$ over the discretised space, parametrised by some small step size h. Then we compute a discretised value function F^h with the property that $F^h \to F$ as $h \to 0$.

Given an h, construct a grid

$$\Omega_h = \{0, h, 2h, \dots, 1-h, 1\}^2, \tag{31}$$

over the unit cube. This grid covers a suitable subset of the state space

$$\mathcal{X} := [T^p, T^p + \Delta T] \times [m^p, m^p + \Delta m] \tag{32}$$

where Δm is chosen such that $T^p + \Delta T$ is stable at $m^p + \Delta m$.

Using the ansatz (30) we can define a discrete value function F_t^h over the grid such that $F_t^h \to F_t$ as $h \to 0$ over χ, that is

$$\begin{aligned} F_t^h(T_t, m_t) = \min_{\chi,\alpha} \Bigg(& \left(1 - e^{-\rho\Delta t}\right) \chi^{1-\frac{1}{\psi}} + \\ & e^{-\rho\Delta t} \left(\delta_y(\chi)\, \mathbb{E}_{t,\mathcal{M}(\alpha)} F_{t+\Delta t}^h(T_{t+\Delta t}, m_{t+\Delta t})\right)^{\frac{1-\frac{1}{\psi}}{1-\theta}} \Bigg)^{\frac{1-\theta}{1-\frac{1}{\psi}}} \end{aligned} \tag{33}$$

where

$$\begin{aligned} \delta_y(\chi) &:= \mathbb{E}_t \left[\left(\frac{Y_{t+\Delta t}}{Y_t} \right)^{1-\theta} \right] \\ &= 1 + \Delta t(1-\theta) \left(\varrho + \phi(\chi) - d(T_t) - \frac{\theta}{2}\sigma_k^2 \right) + \mathbb{E}_t\left[o(\Delta t^{\frac{3}{2}})\right]. \end{aligned} \tag{34}$$

and $\mathbb{E}_{t,\mathcal{M}(\alpha)}$ is the expectation with respect to the Markov chain $\mathcal{M}(\alpha)$ over the grid. This can be constructed, given a step size h, as follows. Introduce the

normalising factor

$$Q_t(T, m, \alpha) \coloneqq \left(\frac{\sigma_T}{\epsilon \Delta T}\right)^2 + \left(\frac{\sigma_m}{\Delta m}\right)^2 + h \left|\frac{r(T) + g(m)}{\epsilon \Delta T}\right| + h \left|\frac{\gamma_t^b - \alpha}{\Delta m}\right|. \tag{35}$$

Then the probabilities of moving from a point (T, m) of the grid to an adjacent point are given by

$$p(T \pm h\Delta T, m \mid T, m) \propto \frac{1}{2}\left(\frac{\sigma_T}{\epsilon \Delta T}\right)^2 + h\left(\frac{r(T) + g(m)}{\epsilon \Delta T}\right)^{\pm} \text{ and} \tag{36}$$

$$p(T, m \pm h\Delta m \mid T, m) \propto \frac{1}{2}\left(\frac{\sigma_m}{\Delta m}\right)^2 + h\left(\frac{\gamma_t^b - \alpha}{\Delta m}\right)^{\pm} \tag{37}$$

where $(\cdot)^+ \coloneqq \max\{\cdot, 0\}$ and $(\cdot)^- \coloneqq -\min\{\cdot, 0\}$. One can readily check that this is a well defined probability measure. Finally, the time step is given by

$$\Delta t = h^2 / Q_t(T, m, \alpha), \tag{38}$$

which satisfies $\Delta t \to 0$ as $h \to 0$.

Then, as the aggregator used in (33) converges to f (23) (Epstein and Zin, 1989), the chain described here satisfies the convergence properties outlined in Kushner and Dupuis (2001), we have $F_t^h \to F_t$ as $h \to 0$.

The Markov chain defined above allows to derive $F_t^h(T_t, m_t)$ from the subsequent $F_{t+\Delta t}^h(T_{t+\Delta t}, m_{t+\Delta t})$. This requires a terminal condition $\bar{F}^h(T_\tau, m_\tau) \coloneqq F_\tau^h(T_\tau, m_\tau)$. To derive this, assume that at some point in a far future $\tau \gg 0$, the abatement is free and all emissions are abated, $\gamma^b = \alpha$, such that $\mathrm{d}m = \sigma_m \, \mathrm{d}W_m$. Then we construct an equivalent, control independent, Markov chain $\bar{\mathcal{M}}$ as above for

$$\bar{F}^h(T_t, m_t) = \min_{\chi} \left(\left(1 - e^{-\rho \Delta t}\right) \chi^{1 - \frac{1}{\psi}} + e^{-\rho \Delta t} \left(\delta_y(\chi) \, \mathbb{E}_{t, \bar{\mathcal{M}}} \bar{F}^h(T_{t+\Delta t}, m_{t+\Delta t})\right)^{\frac{1-\frac{1}{\psi}}{1-\theta}} \right)^{\frac{1-\theta}{1-\frac{1}{\psi}}}. \tag{39}$$

This is now a fixed point equation for $\bar{F}$ which can be solved by value or policy

function iteration.

C Calibration and Parameters

This section summarises the parameters for the preferences, economy, and climate model and discusses the calibration strategy.

The following Table 1 illustrates the preferences parameters used throughout the paper. There is no consensus in the literature on preference parameters. In line with previous literature focusing on recursive preferences, I set relative risk aversion $\theta = 10$ (Ackerman, Stanton and Bueno, 2013; Crost and Traeger, 2013; Lontzek et al., 2015) and the time preference parameter $\rho = 1.5\%$ (Nordhaus, 2014). There is no consensus on whether the elasticity of intertemporal substitution ψ ought to be larger or smaller than unity, with the aforementioned papers using values $\psi \in [0.75, 1.5]$. In this paper, I use $\psi = 1.5$ for the benchmark model and test the robustness of the results to $\psi = 0.75$.

Preferences		
ρ	1.5%	Time preference
θ	10	Relative risk aversion
ψ	1.5	Elasticity of intertemporal substitution

Table 1

Table 2 summarises the parameters of the economy model.

To abate a fraction ϵ of emissions vis-a-vis the BAU scenario requires a fraction

$$\beta(\varepsilon) = \varepsilon^2 \omega_0 e^{-\omega_r t} \tag{40}$$

of GDP. Following (Nordhaus, 2017), we assume that abating all emissions ($\epsilon = 1$) in 2020 costs 11% of GDP while doing so in 2100 costs 2.7% of GDP. This yields the calibrated ω_0 and ω_r.

Table 3 summarises the parameters of the climate model.

Economy		
ω_0	11%	GDP loss required to fully abate today
ω_r	2.7%	Rate of abatement cost reduction
ϱ	0.9%	Growth of TFP
κ	6.32%	Adjustment costs of abatement technology
δ_k	0.0116	Initial depreciation rate of capital
ξ	0.00026	Coefficient of damage function
ν	3.25	Exponent of damage function
A_0	0.113	Initial TFP
Y_0	75.8	Initial GDP
σ_k	0.0162	Variance of GDP
τ	500	Steady state horizon

Table 2

Climate		
T_0	288.56 [K]	Initial temperature
T^{p}	287.15 [K]	Pre-industrial temperature
M_0	410 [p.p.m.]	Initial carbon concentration
M^{p}	280 [p.p.m.]	Pre-industrial carbon concentration
N_0	286.65543 [p.p.m.]	Initial carbon in sinks
σ_T	1.5844	Volatility of temperature
S_0	342 [W / m²]	Mean solar radiation
ϵ	15.844 [J / m² K year]	Heat capacity of the ocean
η	$5.67e-8$	Stefan-Boltzmann constant
G_1	20.5 [W / m²]	Effect of CO_2 on radiation budget
G_0	150 [W / m²]	Pre-industrial GHG radiation budget

Table 3

Non-linearity		
ΔT	1.8 [K]	temperature inflection point
λ_1	31%	Initial radiation reflected
$\Delta\lambda$	.	.

D Stochastic Tipping Benchmark Model

This appendix introduces a benchmark model with stochastic tipping. The stochastic tipping model is a widely used in the economic literature to approximate tipping points in the climate dynamics (e.g. Hambel, Kraft and Schwartz 2021). Comparing the model developed in this paper with the stochastic tipping model allows us to determine if and how the optimal abatement differ and, as a consequence, what the approximation misses.

To establish a meaningful benchmark, I will assume that the contribution of temperature to forcing (9) is given by

$$r_T^s(T) := S_0(1-\lambda_1) - \eta\sigma T^4. \tag{41}$$

This model has no tipping point as $\lambda(T) \equiv \lambda_1$. Stochastic tipping, as commonly modelled in the literature, is introduced as a jump process J with arrival rate $\pi(T)$ and intensity $\Theta(T)$, both increasing in temperature. Intuitively, as temperature rises, the risk of tipping $\pi(T)$ and the size of the temperature increase $\Theta(T)$ grow. Then temperature dynamics in the Stochastic Tipping model follow

$$\epsilon\,\mathrm{d}T = \big(r^s(T) + g(m)\big)\,\mathrm{d}t + \sigma_x\,\mathrm{d}w^s + \Theta(T_t)\,\mathrm{d}N\,. \tag{42}$$

Following Hambel, Kraft and Schwartz (2021), the calibrated arrival rate and temperature increase are calibrated as

$$\pi(T) = -\frac{1}{4} + \frac{0.95}{1+2.8e^{-0.3325(T-T^{\mathrm{P}})}} \text{ and} \tag{43}$$

$$\Theta(T) = -0.0577 + 0.0568(T-T^{\mathrm{P}}) - 0.0029(T-T^{\mathrm{P}})^2. \tag{44}$$